Forschungszentrum Karlsruhe
Technik und Umwelt
Wissenschaftliche Berichte
FZKA 5862

Evaluation of Corrections for Spherical-Shell Neutron Transmission Experiments by the Monte-Carlo Technique

B. V. Devkin, U. Fischer, F. Kappler, M. G. Kobozev, U. von Möllendorff, S. P. Simakov

Institut für Neutronenphysik und Reaktortechnik
Projekt Kernfusion

Dezember 1996

Forschungszentrum Karlsruhe
Technik und Umwelt
Wissenschaftliche Berichte
FZKA 5862

Evaluation of Corrections for Spherical-Shell Neutron Transmission Experiments by the Monte-Carlo Technique

B.V. Devkin[1], U. Fischer, F. Kappler, M.G. Kobozev[1], U. von Möllendorff and S.P. Simakov[1]

Institut für Neutronenphysik und Reaktortechnik
Projekt Kernfusion

1 Institute of Physics and Power Engineering, 249020 Obninsk, Kaluga region, The Russian Federation

Forschungszentrum Karlsruhe GmbH, Karlsruhe
1996

Forschungszentrum Karlsruhe GmbH
Postfach 3640, 76021 Karlsruhe

ISSN 0947-8620

Abstract

The influence of some experimental factors on the measured quantities in neutron spherical-shell transmission benchmark experiments was estimated by simulating the corresponding components of the set-up (materials near the neutron source, collimator and shield of the detector etc.) as well as the specific measuring technique (time-of-flight spectrometry) in Monte-Carlo calculations. The calculations were performed by the MCNP code with nuclear data from the EFF-1 and FENDL-1 libraries. The corrections describing the effects of several distinct experimental details were evaluated.

Berechnung von Korrekturen für Neutronen-Kugelschalentransmissions-Experimente mit der Monte-Carlo-Methode

Zusammenfassung

Der Einfluß einiger experimenteller Einzelheiten auf die Meßgrößen bei Neutronen-Kugelschalentransmissionsexperimenten zur Kerndatenüberprüfung wurde abgeschätzt, indem die entsprechenden Bestandteile der Anordnung (Material nahe der Neutronenquelle, Kollimator und Abschirmung des Detektors u.a.) sowie die spezifische Meßmethode (Flugzeitspektrometrie) in Monte-Carlo-Rechnungen simuliert wurden. Die Rechnungen wurden mit dem Programm MCNP und Kerndaten der Bibliotheken EFF-1 und FENDL-1 durchgeführt. Es wurden Korrekturen bestimmt, die die Auswirkungen der verschiedenen Details jeweils getrennt beschreiben.

1. INTRODUCTION

To obtain experimental data with the maximum possible exactness, a careful estimate of the influence of various experimental details on the measured quantities is generally needed. In neutronics experiments such corrections are often connected with neutron scattering on matter surrounding the neutron source, the exact configuration of the sample under investigation, the detector shielding and others. A very powerful tool is the simulation of the experimental setup and measuring procedure in three-dimensional Monte Carlo transport calculations. By varying the computational model stepwise from a simplified to the most accurate one, the influence of every experimental factor can be analyzed and estimated.

In the present work such a study was made for the task of measuring the neutron leakage flux from spherical iron shells by the time-of-flight (TOF) technique [1].

2. EXPERIMENT

The actual experimental set-up is shown in Fig.1. Short bursts (2 ns) of 14-MeV neutrons were produced by a pulsed neutron generator via the T(d,n) reaction. A titanium-tritium target was located at the center of the spherical iron shell. The spectral neutron flux leaking from the outer surface of the shell was measured by a fast scintillator detector at a flight path of either 4 or 7 m. The detector was installed either in a heavy shield or in a lead house behind a concrete wall having a hole. For background measurements, a 1 m long iron shadow bar was placed between the spherical shell and the detector. A long counter and a pulse monitor (a fast plastic scintillator positioned close to the source) were used to monitor the yield of 14-MeV neutrons and the pulse shape and repetition period of the neutron source respectively.

The target assembly design is shown in Fig. 2. The assembly is a conical tube with wall thickness of 0.5 mm. The titanium-tritium target on a copper radiator (∅11mm × 0.8mm) was placed at the closed end. The deuteron beam went through a ∅8mm diaphragm. The alpha particles produced in the T(d,n)^{4}He reaction were detected by a silicon surface barrier detector after passing through a ∅1mm collimator.

Five different iron spheres were investigated. The spheres no. 1 and 4 are shown in Fig. 3. The parameters of the spheres - outer (R) and inner (r) radii and wall thickness (t=R-r) - are listed in Table 1. Each sphere has a radial hole for accommodating the deuteron beam drift tube and target (Fig. 3). The configurations (radius R_h and length L_h) of

Table 1. Configuration of spherical iron shells

No.	Sphere Sizes, cm			Hole Configuration, cm	V_h/V, %
	R	r	t	$R_h(L_h)$	
1	4.5	2.0	2.5	2.0(2.5)	10.6
2	12.0	4.5	7.5	3.2(4),3.0(3.5)	3.3
3	12.0	2.0	10.0	3.2(4), 3.0(3.5), 2.0(2.5)	3.7
4	20.0	1.9	18.1	2.5(10.3), 1.9(7.8)	0.9
5	30.0	2.0	28.0	4(7), 2.5(7.8), 2.0(13.2)	0.6

these holes and the ratios of hole volume to sphere volume (V_h/V) are also listed in Table 1. Spheres no. 4 and 5 were kindly made available by another team of the Obninsk Institute [3].

The energy-dependent neutron detector efficiency is one of the important parameters affecting the accuracy of the final results. This is why much attention was paid to it in the experiment and in the calculation. It was experimentally determined by measuring the spectrum of neutrons from the spontaneous fission of ^{252}Cf, which is known in the range 0.1MeV-10MeV with 3% accuracy [4]. A drawing of the Cf fission chamber is shown in Fig. 4. The instant of every disintegration (about 5×10^5 per second) was detected by registration of the fission fragment ionization pulse. A discriminator threshold suppressed low amplitude pulses from alpha particles. The appropriately delayed ionization pulse was used as a stop pulse in the time-of-flight measurement and for the total counting of fission events.

More details are found elsewhere [1, 2].

3. MONTE CARLO SIMULATION OF THE EXPERIMENT

Three-dimensional Monte Carlo simulations of the experiment have been made with the MCNP-4.2 code [5] on IBM RISC Series computers at Karlsruhe. The nuclear data for the calculations were taken from the European Fusion File EFF-1 [6] and the Fusion Evaluated Nuclear Data Library FENDL-1 [7].

3.1 Time-of-flight measuring technique in case of bulk samples

The time-of-flight method presupposes a strict relation between the neutron energy E, the sample-detector distance L and the flight time t:

$$E = mc^2 (1/\sqrt{1-(L/ct)^2} - 1) \approx (72.3 \cdot L[\mathrm{m}]/t[\mathrm{ns}])^2 ,$$

where: m - neutron mass,

c - light velocity in vacuum.

This equation is fulfilled if the dimensions of source, sample and detector and the source-sample distance can be neglected in comparison with the detector-sample distance. However, in benchmark experiments of the spherical-shell transmission type, the size of the sample assembly in general is not negligible since the ratio of the sphere radius to the sphere-detector distance is 1-5%.

The consequences of this experimental geometry can be evaluated because the MCNP code calculates both the energy and the time of arrival of a neutron at the detector. With proper, detailed modeling, the calculations take into account the real geometry of the experiment and the real travel time that the neutron spends on its way from the source via the sample sphere to the detector. The time distribution of the neutrons arriving at the detector position, referred to the start of the neutron from the source as zero time, can then be converted to an energy spectrum using the above equation. This procedure, therefore, is a simulation of the time-of-flight experiment together with its data reduction procedure. The leakage spectrum $L(E(t))$ obtained in this way ('time-dependent Monte-Carlo technique') can be compared with the energy distribution $L(E)$ of the neutrons calculated directly by the MCNP code, without considering any time relationship ('time-independent Monte-Carlo technique'). This results in a correction function $C_t(E)=L(E)/L(E(t))$, which should be multiplied to an experimental spectrum before comparing it with a Monte-Carlo spectrum calculated in the time-independent way. The energy dependence of $C_t(E)$ is shown in Fig. 5 for the five iron shells. It is seen that this correction will increase the measured leakage spectrum in the energy range 0.5 - 5 MeV but decrease it at energies less than 0.3 MeV. The amount of the correction depends on shell thickness. For the largest sphere, it varies between -20% and +10%.

Time delays of neutrons, due to longer distances covered within the sphere by scattering, result in a further effect, an apparent shift of resonances to lower energies in the spectrum obtained by the time-dependent technique. In Fig. 6, which shows $L(E)$ and $L(E(t))$ separately for shells 1 and 5, such a shift is clearly noticeable for shell 5 in the en-

energy range below 1 MeV. This shift was originally seen in our experimental data, and it led us to perform the above investigation.

3.2 Corrections for non-spherical effects

Many transport codes (e.g., ANISN, ONEDANT, ANTRA-1 etc.) use the one-dimensional (spherical) approximation. Such calculations would be immediately comparable only with the results of an ideal benchmark experiment which is spherically symmetric in every respect. The real experiment deviates from spherical symmetry because of:

1. the beam hole (channel) in the shell,
2. the non-spherical matter distribution of the target assembly,
3. the dependence of both source neutron energy and differential source strength (i.e., yield per element of solid angle) on the reaction angle.

The experimental data have to be corrected for these effects before they can be compared with 1-dimensional code results. Results for these 3 effects are discussed in the following.

1. The influence of the hole has been estimated by comparison of leakage spectra calculated for shells without ($L(E)$) and with ($L_h(E)$) the hole. In the calculation the detector was placed at distance 6.8 m and angle 8° relative to the deuteron beam (see Fig. 1). The corresponding correction function $C_h(E) = L(E)/L_h(E)$ is shown in Fig. 7 for four of the iron shells. It is seen that the correction correlates with the relative hole volume and has a maximum value of 20% for the smallest shell, no. 1.

   The effect of the hole is particularly significant for 14-MeV neutrons. In Fig. 8 the calculated angular distributions of the 14-MeV neutron group are shown. It is seen that the leakage flux in this energy group gives information about the transmission of source neutrons through the spherical shell if it is measured in the forward hemisphere, whereas it is seriously affected by the hole in backward directions beyond 150°. Near 180° the 14-MeV flux with an iron shell in place is even increased over the 14-MeV flux from the bare source. This is plausible, since the detector in this case would see, through the hole, the direct source neutrons plus additional neutrons elastically scattered towards itself.

2. The distribution of matter around the target leads to an angle-dependent flux attenuation of the uncollided (14-MeV) neutrons as well as to spectral modifications. For

the target assembly described above, the calculated angular distribution of 14-MeV neutrons is shown by the dashed curve in Fig. 9. The attenuation is strongest (7-10%) at angles close to 90° and 150°, where the material thickness is largest. Nevertheless the total (4π sr integrated) attenuation is relatively small, 2.5%. The dashed curve is identical with the solid curve of Fig. 8 except for the different ordinate scale.

The spectral modification, i.e. the flux of lower-energy neutrons produced by inelastic neutron interactions in the target assembly, is much less dependent on angle, because these processes distribute their product neutrons through the total 4π steradians. It is a reasonable approximation to assume the part below the 14-MeV peak in the spectrum of neutrons entering the sample shell to be isotropic.

3. The T(d,n)^{4}He reaction at deuteron energies below 300 keV is very accurately isotropic in the center-of-mass coordinate frame [8]. The anisotropies of source neutron energy and yield can, therefore, be calculated by the kinematic coordinate transformation into the laboratory frame. The resulting angular dependences [9] of both of these quantities for our case are shown by the solid curves in Fig. 9. The yield anisotropy amounts to about ±6%.

The experimental and Monte-Carlo calculated energy spectra of the bare neutron source are shown in Fig. 10 for the detector angle 8°. Besides the 14-MeV peak there is a broad low energy (0.2 - 5 MeV) bump, which is caused by non-elastic scattering of neutrons on the target assembly. The discrepancies between the experimental and calculated spectra may be explained by underestimation of direct inelastic scattering in the evaluated nuclear data file used (EFF-1). As mentioned above, the low energy part of the source spectrum is assumed to be independent of emission angle, whereas the mean energy of the '14-MeV' peak is a function of angle as shown in Fig. 9.

3.3. Correction for neutron detector efficiency calibration

As Fig. 3 shows, the Cf-252 fission chamber was made from thin and low mass materials. Nevertheless, a distortion of its spectrum due to neutron scattering by the chamber materials is still possible. To estimate this effect, the neutron interaction with the Cf chamber (Fig. 3) was simulated by Monte-Carlo calculations. Fig. 11 shows the ratios of several spectra calculated for the detector location to the pure Cf-252 emission spectrum taken from Ref. [4]. The influences of different factors were analyzed.

The solid line shows the distortions of the Cf spectrum resulting only from scattering of neutrons on the chamber materials. The long-dashed line shows the influence of the air (the distance between Cf chamber and detector is about 5 m), which results in an attenuation of the flux above 3 MeV and an increase below 3 MeV. The short-dashed line shows the scattering of neutrons on the walls of a 1m long concrete collimator (see Fig. 1), which increases the effective solid angle and softens the spectrum by scattering on the collimator materials.

During efficiency measurements, the detector views not only the TiT-target assembly but also the deuteron beam tube including massive parts such as quadrupole lenses and flanges (Fig. 1). Simulation of these elements shows that the contribution from beam tube scattering at the detector location is negligible (dotted curve).

All or some of these effects should be taken into account if the detector efficiency is theoretically calculated or measured in conditions different from those where the neutron leakage spectra are measured. In our case, there is only one factor (influence of chamber material) which we have to take into account, since the influence of air and collimator is the same in efficiency and neutron leakage spectra measurements. It is seen that neutron scattering on the chamber materials changes the flux by up to 4% in the low energy part. This correction was applied in processing our experimental data.

4. CONCLUSIONS

Three-dimensional Monte-Carlo simulations of spherical-shell neutron transmission benchmark experiments permitted us to analyze the influence of different experimental factors on the measured quantities. The distortion of the leakage neutron spectrum introduced by the time-of-flight technique, i.e. by neglecting neutron trajectories longer than the straight line source-detector and neutron energy changes on the way, was estimated. The contributions from neutron interaction with the neutron source assemblies (TiT target

assembly, Cf-252 fission chamber), with the room air and with the detector collimator were calculated as well. In view of one-dimensional transport calculations, which are sometimes used for comparison with such experiments, the effects of the inevitable deviations from perfect spherical symmetry were also investigated.

It was shown that effects of these kinds may modify the flux in certain regions of the leakage spectrum by as much as 10-20%, exceeding the experimental uncertainty. To improve the accuracy of the experimental results, corresponding corrections should be calculated for every specific experiment configuration and applied to the measured data.

ACKNOWLEDGEMENT

This work has benefitted from support towards travel and staying expenses obtained on the basis of the Agreement on Scientific-Technological Cooperation in the Peaceful Utilization of Nuclear Energy between the Federal Ministry of Education, Science, Research and Technology of the Federal Republic of Germany and the Ministry of Atomic Energy of the Russian Federation.

REFERENCES

1. S. P. Simakov, B. V. Devkin et al., in: Fusion Technology 1992, ed. by C. Ferro et al., vol. 2, p. 1489, Elsevier Science, Amsterdam, 1993
2. B. V. Devkin, M. G. Kobozev et al., in: Fusion Technology 1994, ed. by K. Herschbach et al., vol. 2, p. 1357, Elsevier Science, Amsterdam, 1995
3. L. A. Trykov, Yu. I. Kolevatov et al., report FEI-1730, Obninsk, 1985
4. W. Mannhart, in: report IAEA-TECDOC-410, Vienna, 1987, p.158
5. J. F. Briesmeister (ed.), report LA-12625-M
6. P. Vontobel, PSI report 107 (1991)
7. S. Ganesan, P. K. McLaughlin, report IAEA-NDS-128, Vienna, 1994
8. H. Liskien and A. Paulsen, Nucl. Data Tables 11 (1973) 569
9. J. Chikai et al., in: report IAEA-TECDOC-410, Vienna 1987, p. 296

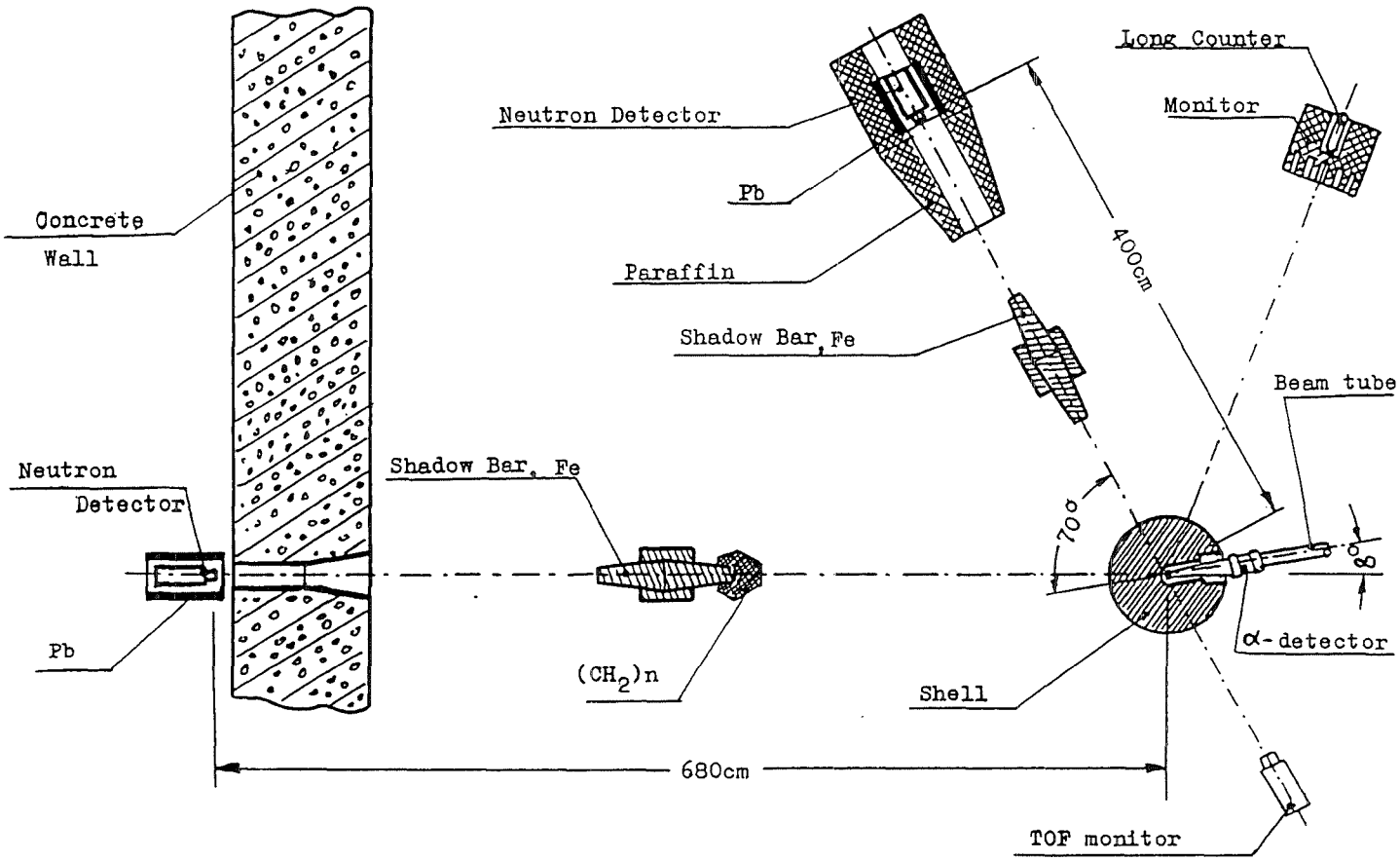

Fig. 1. Lay-out of experiment for measuring the neutron leakage spectra at short (4.0m) and long (6.8m) flight path.

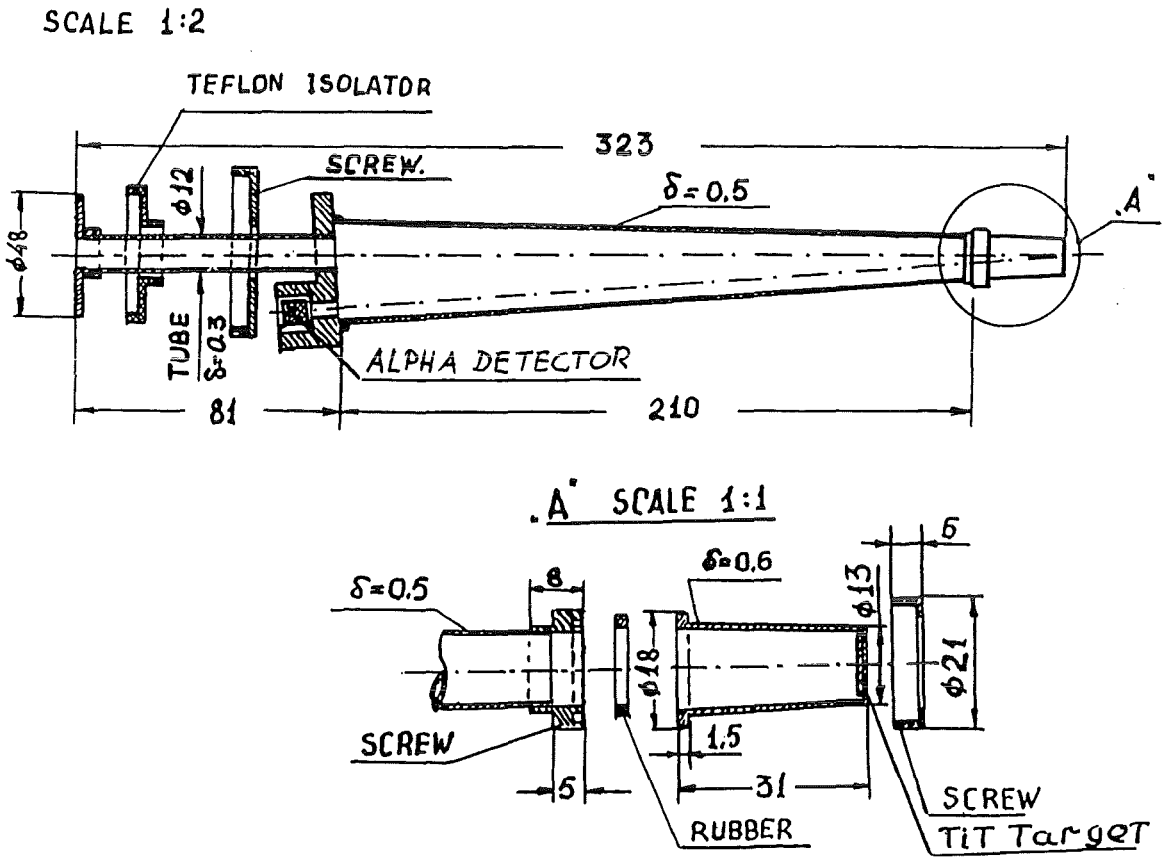

Fig. 2. Design of ion beam tube and tritium target assembly

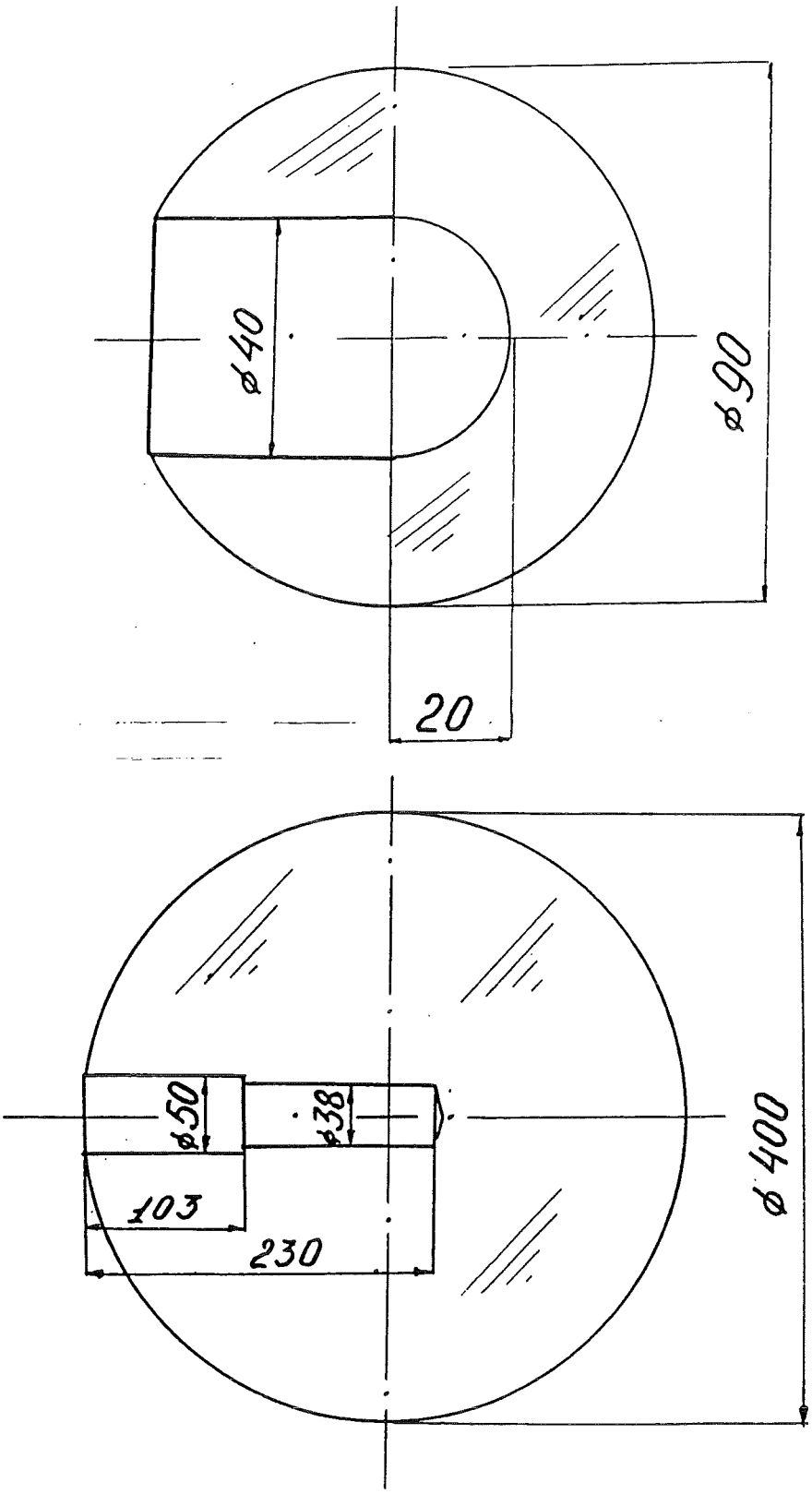

Fig. 3. Design of iron spheres No 1 and 4

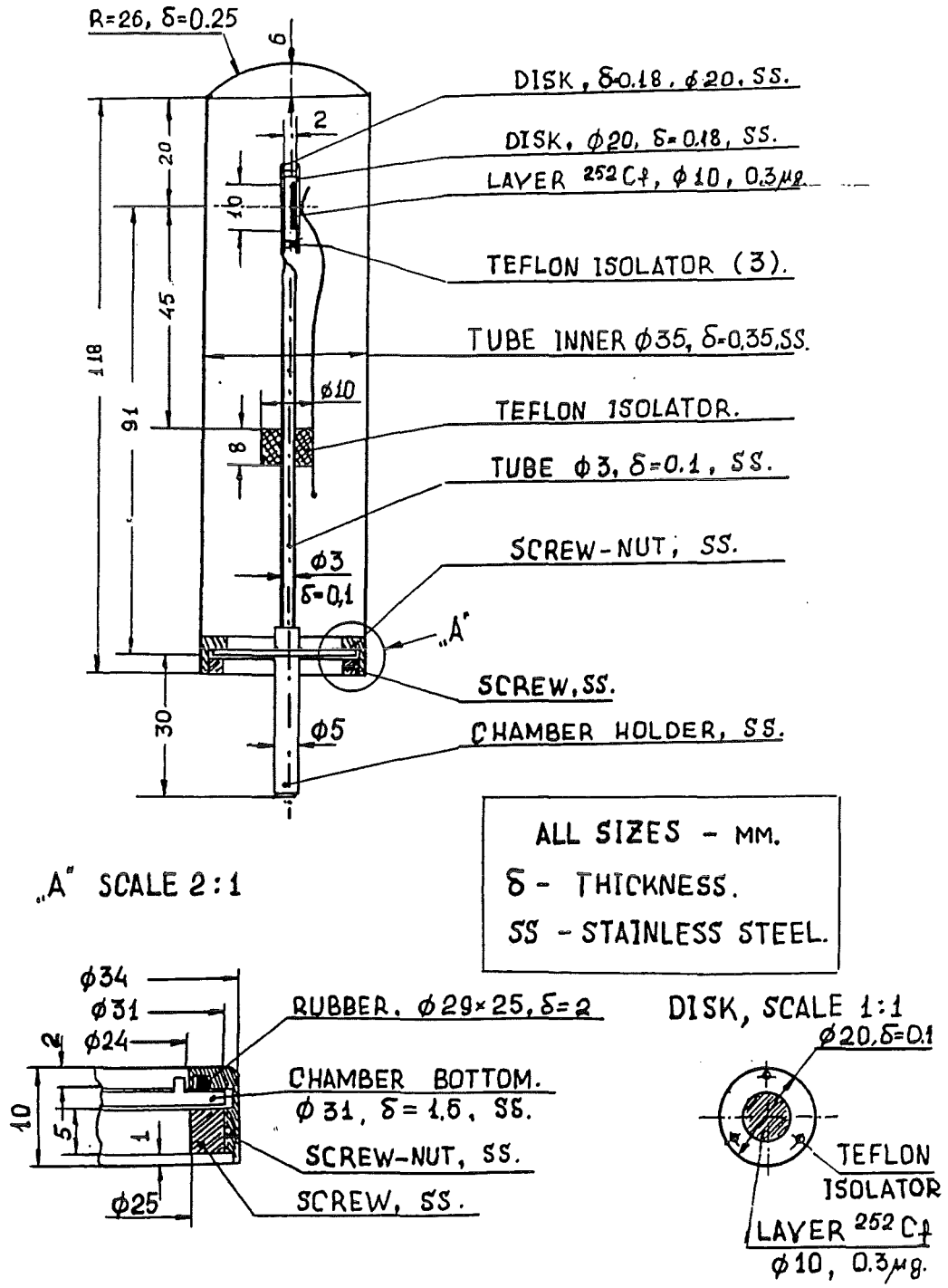

Fig. 4. Design of Cf-252 fission chamber used for energy calibration

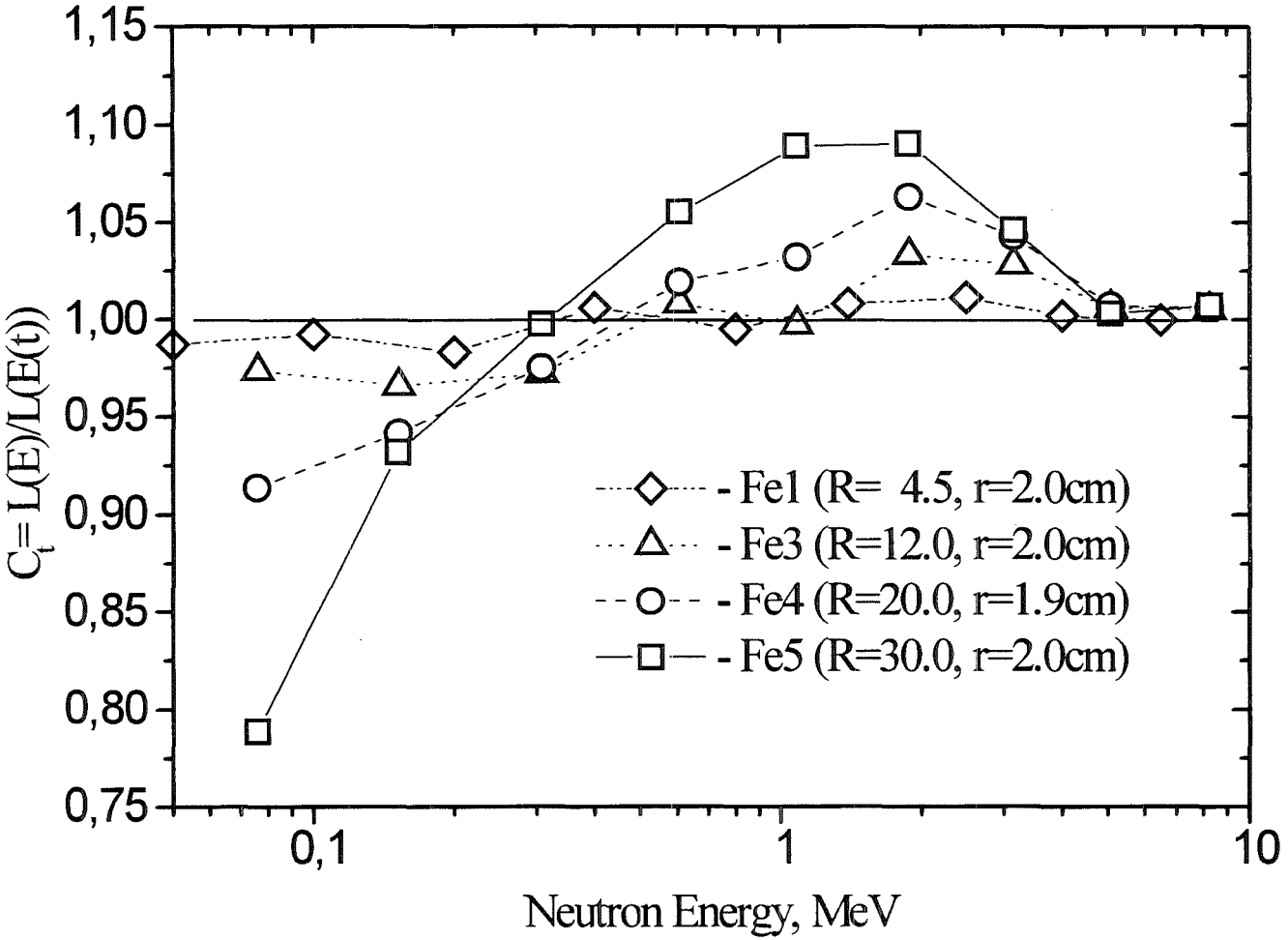

Fig. 5. Correction for time-of-flight measuring technique

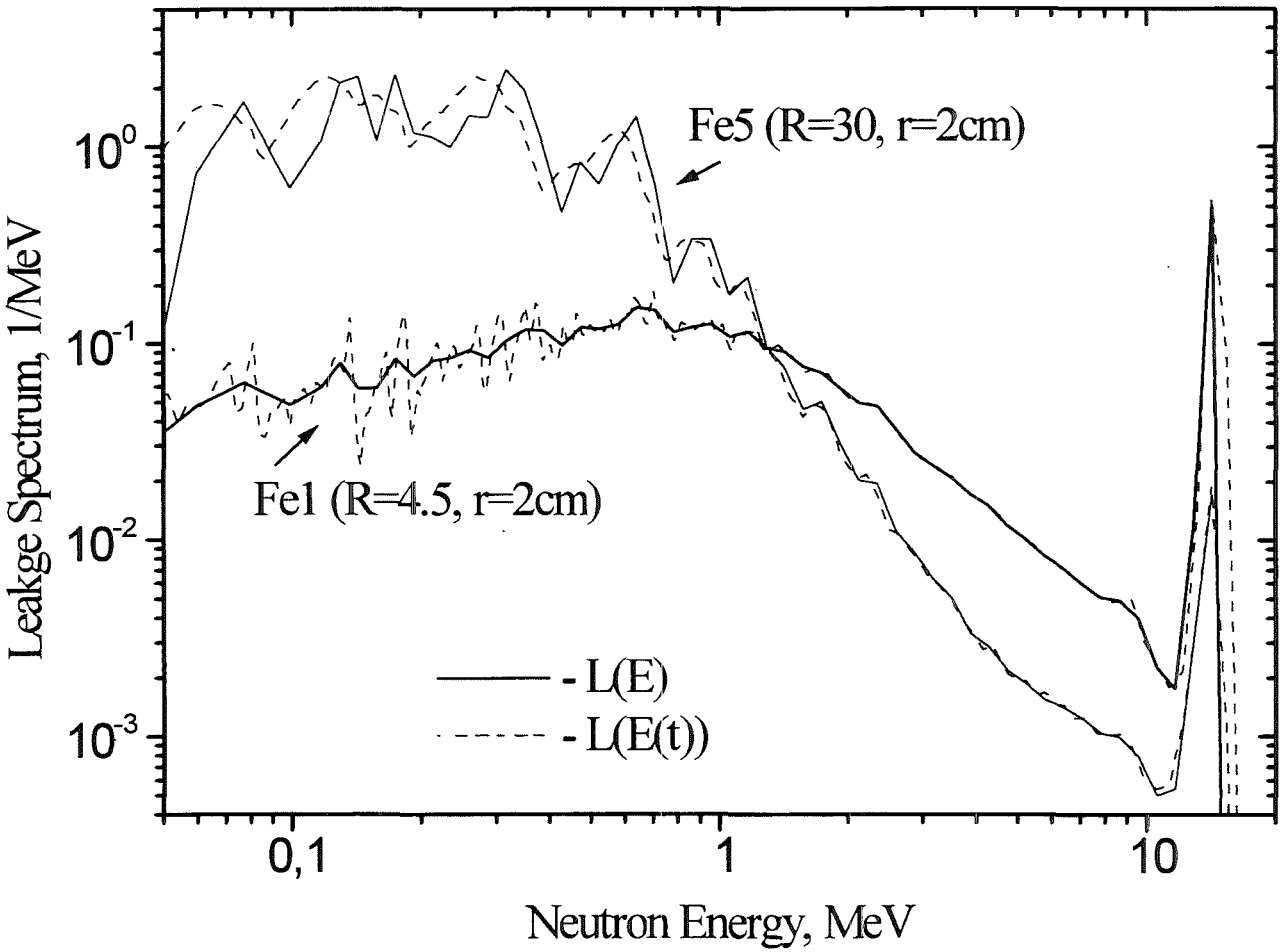

Fig. 6. Comparison of time dependent and time independent calculations of leakage spectra

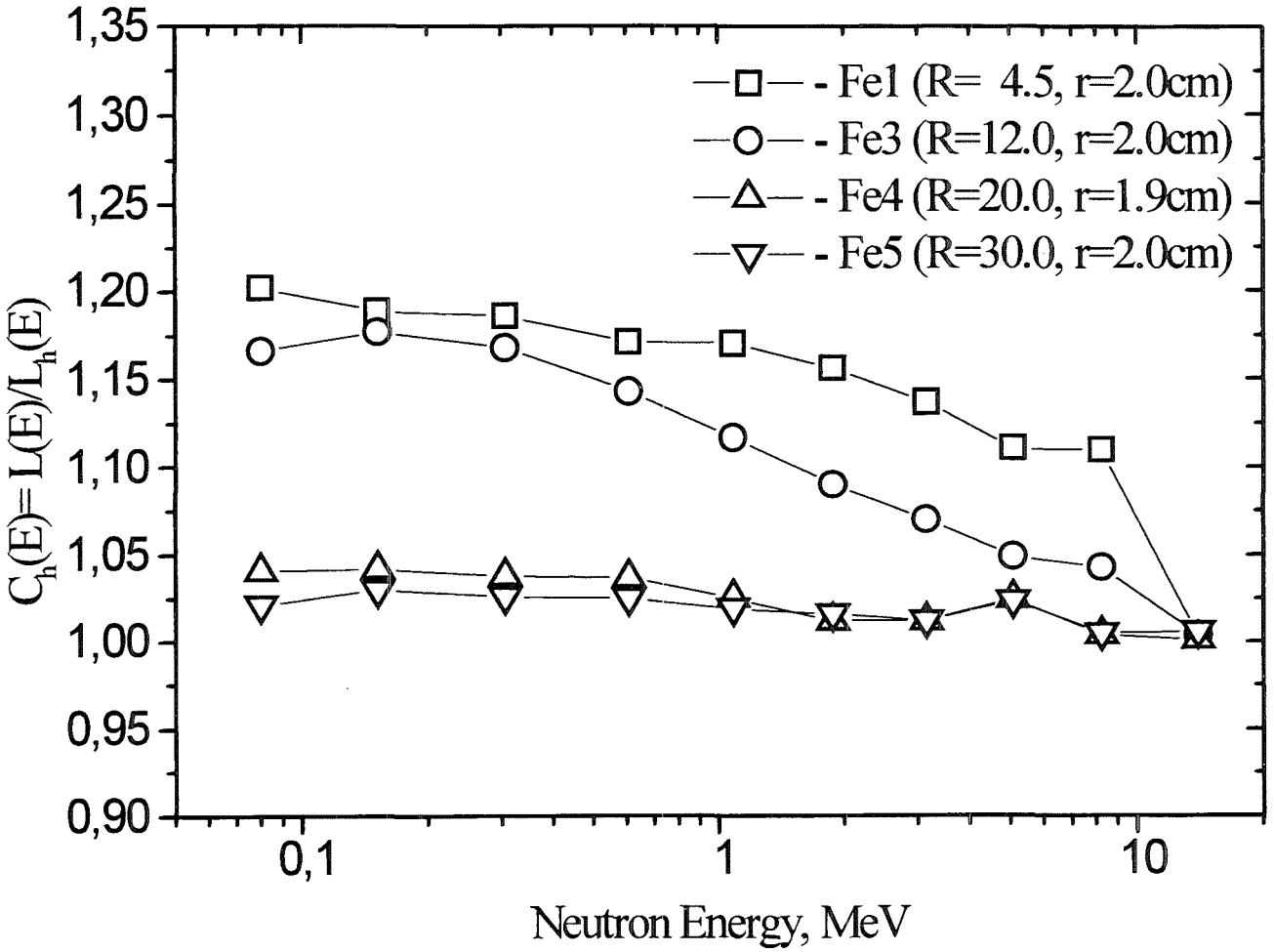

Fig. 7. Correction for beam hole in shell

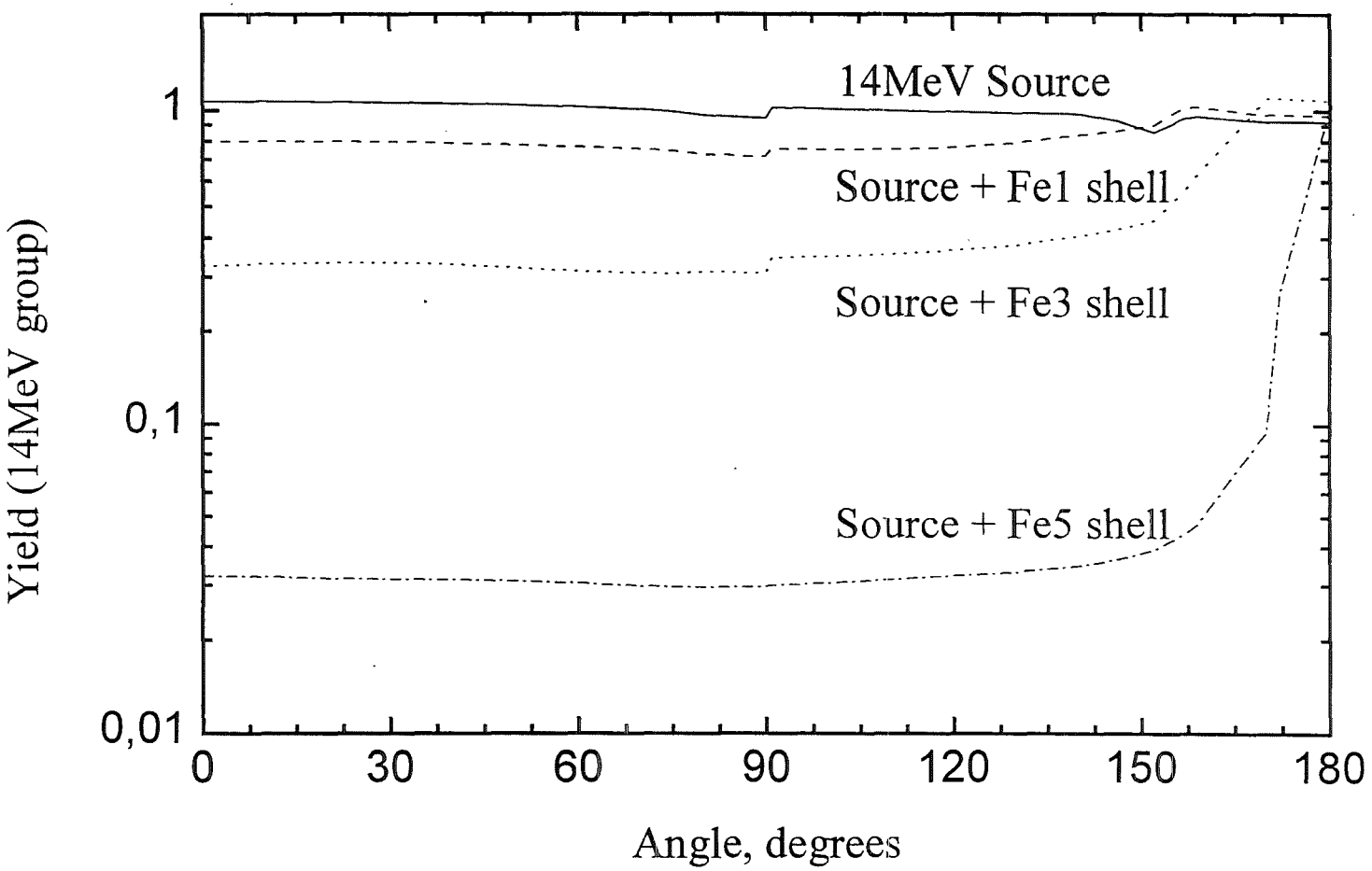

Fig. 8. Angular distributions of 14-MeV group neutrons

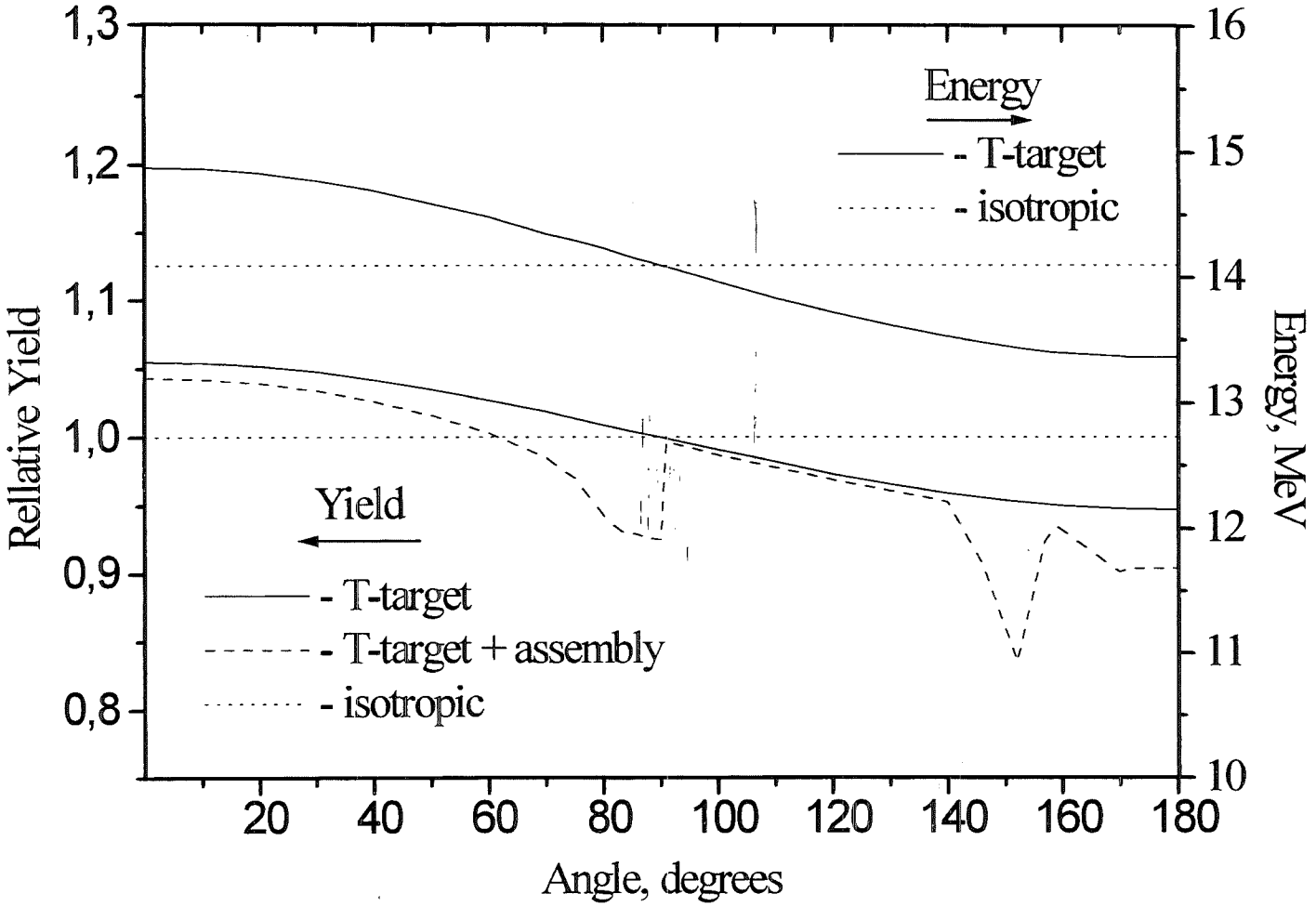

Fig. 9. Angular and energy distributions of '14-MeV' neutrons in the laboratory coordinate frame ('T target' refers to a thick target with an incident 250-keV deuteron beam)

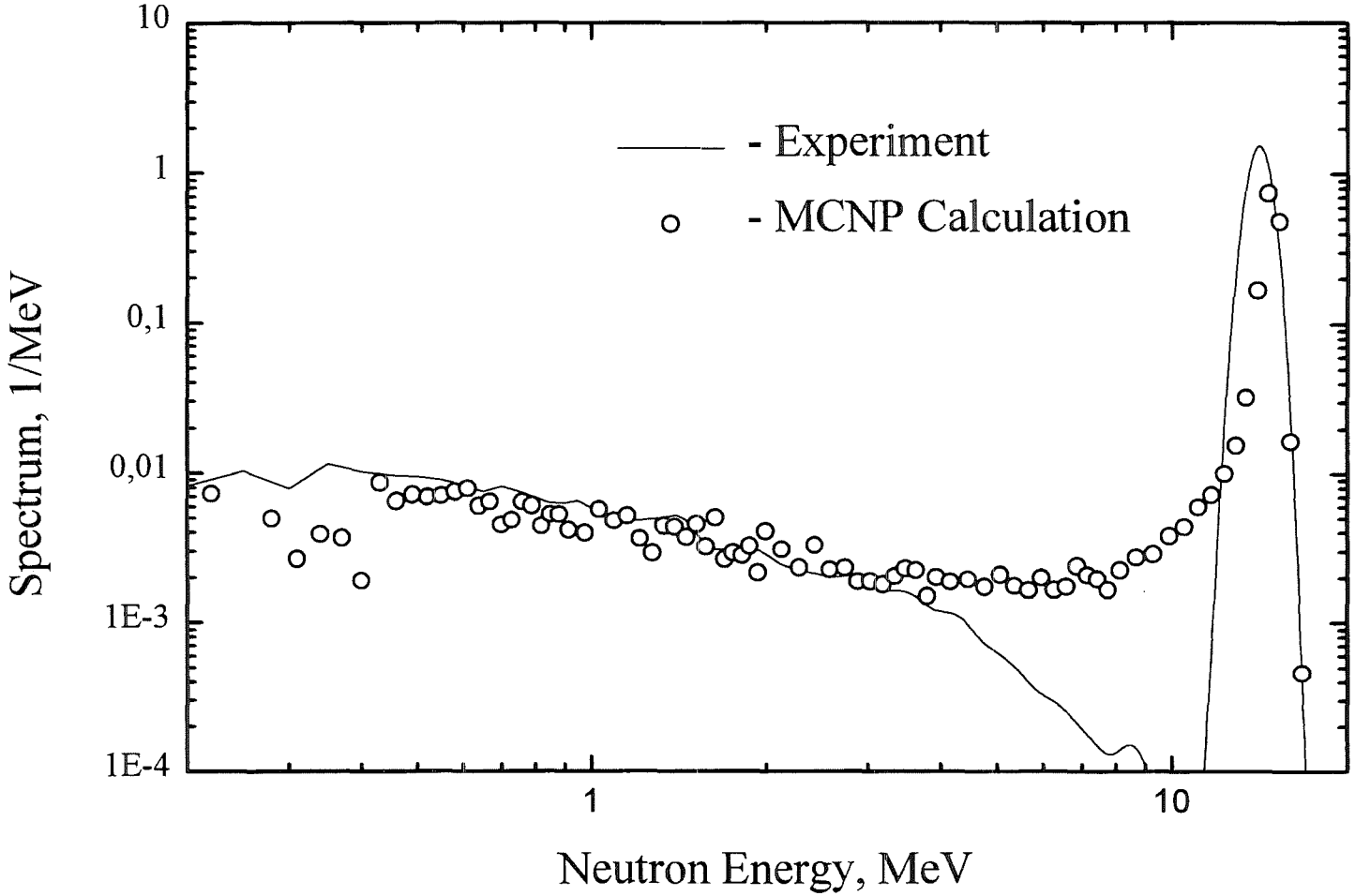

Fig. 10. Energy spectrum of neutrons emitted by target assembly at emission angle 8°
(Calculated spectrum based on EFF-1 data)

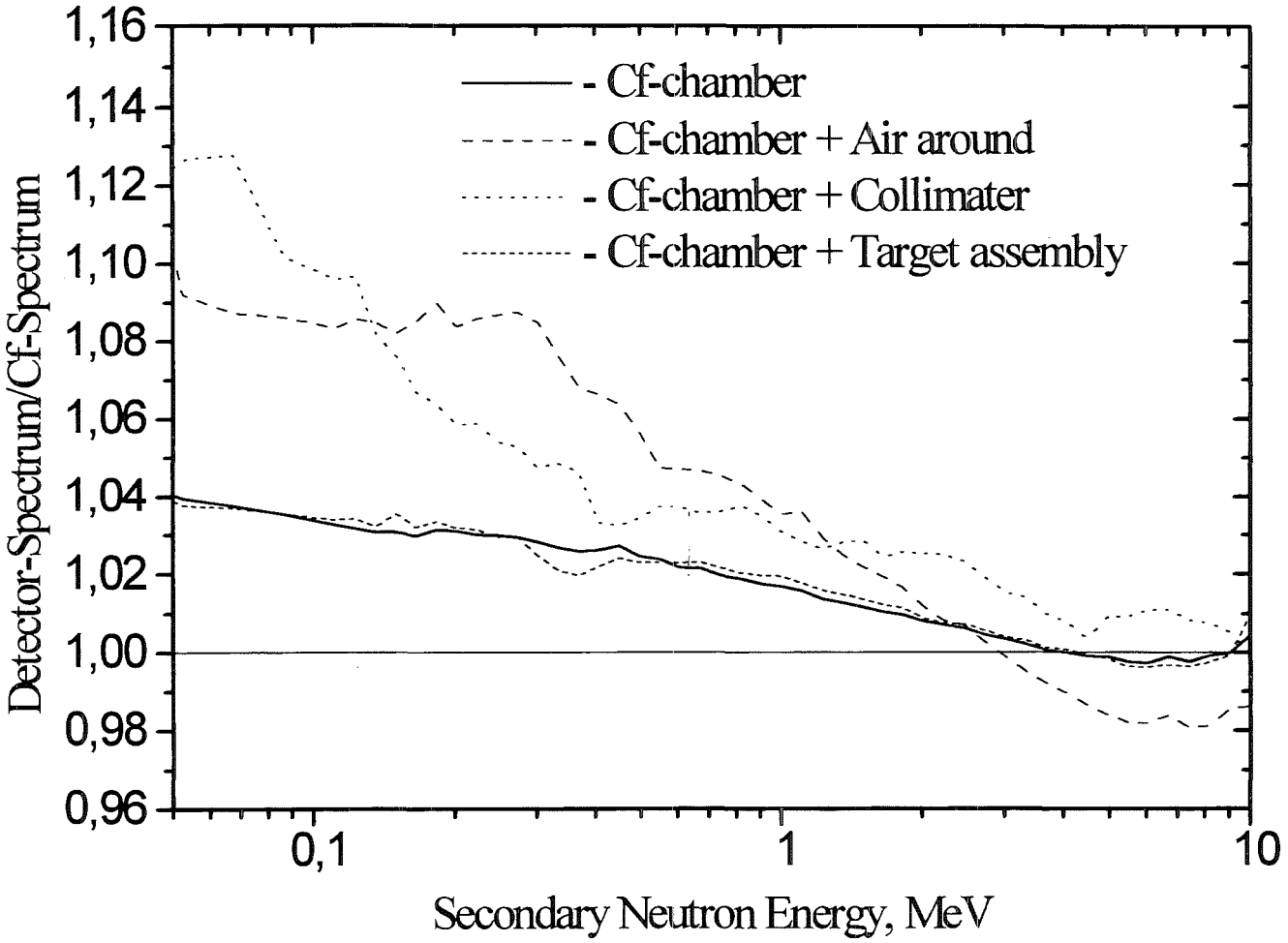

Fig. 11. Influence of fission chamber, air, collimator and target assembly on ^{252}Cf spectrum